frontiers | Frontiers in Materials

TYPE Original Research
PUBLISHED 29 January 2025
DOI 10.3389/fmats.2025.1539929

Check for updates

OPEN ACCESS

EDITED BY
Xiangming Zhou,
Brunel University London, United Kingdom

REVIEWED BY
Cong Lu,
Southeast University, China
Yanshuai Wang,
Shenzhen University, China

*CORRESPONDENCE
Fengxia Xu,
ll6918tofb204@163.com

RECEIVED 05 December 2024
ACCEPTED 14 January 2025
PUBLISHED 29 January 2025

CITATION
Wang H, Xu F, Liu Z, Zhong S, Xing E, Ye Y, Zhao Y and Li C (2025) Preparation and carbon emission analysis of high-performance pavement concrete using waste gypsums.
Front. Mater. 12:1539929.
doi: 10.3389/fmats.2025.1539929

COPYRIGHT
© 2025 Wang, Xu, Liu, Zhong, Xing, Ye, Zhao and Li. This is an open-access article distributed under the terms of the Creative Commons Attribution License (CC BY). The use, distribution or reproduction in other forums is permitted, provided the original author(s) and the copyright owner(s) are credited and that the original publication in this journal is cited, in accordance with accepted academic practice. No use, distribution or reproduction is permitted which does not comply with these terms.

Preparation and carbon emission analysis of high-performance pavement concrete using waste gypsums

Hui Wang[1], Fengxia Xu[2]*, Zhen Liu[1], Shunjie Zhong[3], Enkuo Xing[1], Yongbin Ye[4,5], Yan Zhao[6] and Chenjiang Li[7]

[1]Cangzhou Qugang Expressway Construction Co. Ltd., Cangzhou, China, [2]College of Biological and Environmental Engineering, Tianjin Vocational Institute, Tianjin, China, [3]Fujian Zhanglong Construction Investment Group Co. Ltd., Zhangzhou, China, [4]Fujian Xingyan Construction Group Co. Ltd., Zhangzhou, China, [5]Fujian Rongguan Construction Engineering Co. Ltd., Zhangzhou, China, [6]China MCC22 Group Corporation Ltd., Tangshan, China, [7]State Key Laboratory of Hydraulic Engineering Intelligent Construction and Operation, Tianjin University, Tianjin, China

This study explores the potential of waste gypsum, specifically phosphogypsum (PG) and desulfurization gypsum (DG), as alternative materials in supersulfated cement-based concrete (SSCC) for low-carbon road construction. The research comprehensively investigates the effects of PG and DG on the mechanical properties, corrosion resistance, and water resistance of SSCC. Additionally, the hydration kinetics and microstructure of SSC are analyzed through isothermal calorimetry, X-ray diffraction, and scanning electron microscopy. The findings show that PG-modified SSCC outperforms DG-modified SSCC, with 26.9% and 28% improvements in compressive and flexural strengths, respectively. Both PG and DG contribute to enhanced corrosion resistance, particularly in acidic environments, due to the formation of distinct hydration products compared to traditional concrete. Microstructural analysis reveals denser structures with Ettringite (AFt) and calcium silicate hydrate. Moreover, the hydration process of SSC exhibits low heat release, mitigating cracking risks in outdoor applications. A comprehensive evaluation indicates that PG-modified SSCC not only offers superior mechanical properties but also demonstrates significantly reduced carbon emissions and energy consumption, highlighting its potential as a sustainable material for road concrete.

KEYWORDS

waste gypsums, supersulfated cement, road concrete, corrosion resistance, carbon emissions

1 Introduction

Cement concrete is one of the most widely used building materials (Gartner, 2004), formed by the mixing and hydration of cement, aggregates, water, and admixtures (Mo et al., 2016). It is employed in various types of construction, including pavements (Selvam et al., 2023), bridges (Lantsoght, 2022), tunnels (Lin et al., 2021), underground engineering, civil and industrial buildings (Wang et al., 2023), and hydraulic engineering (Zhang, 2021). Portland cement-based concrete is currently the predominant material for road pavements. In recent years, new materials and technologies have been gradually introduced to enhance the mechanical performance, durability, and environmental sustainability of roads.

Commonly used alternatives include high-performance concrete (HPC) (Xu et al., 2021), asphalt mixtures (Xue et al., 2024), recycled materials, pervious concrete (Akkaya and Çağatay, 2021), and polymer-modified cement-based concrete. However, the extensive use of cement-based concrete has led to increased carbon emissions, contributing to global warming (Intergovernmental Panel on Climate Change, 2022; Li M. et al., 2020). In the context of global efforts to reduce carbon emissions (Blanco, 2022), new requirements have emerged for road pavement concrete. Consequently, reducing the use of Portland cement has become an effective strategy for lowering carbon emissions (Cantini et al., 2021). Research into developing green cementitious materials to replace Portland cement is a key approach to achieving carbon reduction (Jiang et al., 2024; Zhonglin et al., 2024). For example, Wu et al. (2018) developed a low-carbon lime-based cementitious material (LCM) with a compressive strength of 50–60 MPa at 28 days and more than 70 MPa at 180 days, significantly reducing carbon emissions, energy consumption, and environmental impact compared to Portland cement. Similarly, Wang et al. (2024) introduced a low-carbon binder made from fly ash, ground granulated blast furnace slag, steel slag, and desulfurization gypsum, demonstrating reduced energy consumption in its production (Peng et al., 2022; Cui et al., 2024). However, various durability challenges remain before these low-carbon materials can be adopted on a large scale.

Supersulfated cement (SSC) has emerged as an eco-friendly cementitious material (Wu et al., 2021), primarily composed of slag and gypsum (Liu et al., 2020). First proposed by Prof. Kühl in Germany in 1908, SSC typically consists of over 75% slag, 15% gypsum, and 5% Portland cement (Liu et al., 2020; Cabrera-Luna et al., 2024). SSC offers significant advantages in terms of resource conservation and the effective recycling of industrial waste, helping protect natural resources and address the utilization of renewable materials (Jiang et al., 2018; Li et al., 2023). SSC is also renowned for its excellent corrosion resistance, particularly in chloride- and sulfate-rich environments (Pinto et al., 2020a; Pinto et al., 2020b). Cabrera-Luna et al. (2020) studied the corrosion resistance of supersulfated cement concrete (SSCC) based on volcanic pumice and found that the microstructure of SSCC exhibited a matrix with microporosity, where calcium silicate hydrate (C-S-H) and ettringite (AFt) were homogeneously mixed. These hydration products helped immobilize chlorides, improving the durability of steel reinforcement in SSCC exposed to corrosive conditions. Chang et al. (2024) examined the deterioration mechanism of SSC pastes containing phosphogypsum (PG) when exposed to sodium sulfate and hydrochloric acid-sodium sulfate solutions. Findings showed that while Portland cement suffered from swelling and cracking in Na_2SO_4 solution due to the formation of AFt and gypsum, the hydration products in SSC remained stable, exhibiting high resistance to sulfate attack. SSC's superior chemical resistance has led to its widespread use in harsh environments such as marine settings, chemical plants, and sewage treatment plants. Research into SSC applications is ongoing, with studies by Zokaei et al. (2024) exploring its use as a sustainable alternative to Portland cement in engineered cement composites (ECC), and Kazanskaya et al. (2021) investigating its physical and mechanical properties in expanded clay lightweight concrete, which showed increased tensile strength and better cracking resistance.

Despite its potential, large amounts of gypsum remain underutilized (Huang et al., 2020). However, its potential for high-value applications can be realized by using gypsum as a sulfate activator in SSC. Li Y. et al. (2020) noted that desulfurization gypsum (DG) activates slag more slowly but can be accelerated with the addition of electric arc furnace reducing slag (EAFRS). Kang et al. (2024) also explored DG as a sulfate activator for SSC. In addition, many studies have examined the use of phosphogypsum (PG) as a sulfate activator in SSC (Pinto et al., 2020b; Liu et al., 2019; Gracioli et al., 2020).

To address the sustainability challenges in high-performance pavement concrete and improve the utilization of waste gypsum, this research focuses on developing road pavement concrete using SSC as the primary cementitious material. The study evaluates the mechanical performance, corrosion resistance, and water absorption of gypsum-modified SSC, comparing it to traditional Portland cement-based concrete. The hydration mechanisms of PG-modified SSC are investigated at the microstructural level using heat of hydration testing, X-ray diffraction (XRD), and scanning electron microscopy (SEM) to analyze the formation of hydration products and their impact on concrete performance. Additionally, carbon emissions, energy consumption, and cost analyses are conducted to assess the long-term viability of SSC. This research aims to provide a scientific foundation for the application of SSC in road engineering and promote its broader use in construction, offering a more eco-friendly, economical, and durable alternative for future road construction projects. Ultimately, it seeks to support the sustainable development of the construction industry.

2 Material and methods

2.1 Raw materials

The cement used in this study was P·O 42.5 Portland cement, sourced from Shenyang, Liaoning Province. The particle size distribution of the cement is shown in Figure 1, with a median particle size of 12.7 μm and a maximum particle size of 31.1 μm. The slag utilized was S95-grade mineral powder. Two types of gypsum were employed in the experiments: desulfurization gypsum (DG) and phosphogypsum (PG). The microstructures of PG and DG were characterized using scanning electron microscopy (SEM), as shown in Figure 2. The results revealed that PG consisted of larger particles with a higher degree of particle aggregation and a more regular, flaky shape, while DG was composed of smaller, spherical particles. The chemical compositions of PG and DG were analyzed using X-ray fluorescence (XRF), and the results are presented in Table 1. It was observed that PG had a lower CaO content compared to DG, but a higher SO_3 content. Additionally, the specific surface areas of PG and DG were found to be 2.3 and 3.19 m^2/g, respectively.

2.2 Preparation of specimens

The mixing proportions for the specimens are shown in Table 2. Coarse aggregate (CA), fine aggregate (FA), and polycarboxylic acid water reducer (SP) were used in the preparation. The concrete mixing process was carried out using a horizontal rail mixer as

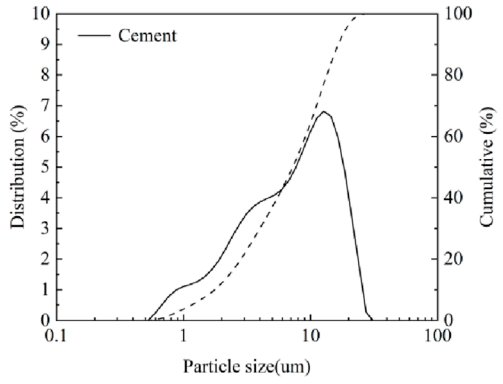

FIGURE 1
The particle size distribution of cement.

follows: First, the sand, coarse aggregate, and cementitious materials, which had been homogenized according to the specified mix ratio, were added to the concrete mixer for an initial mixing period of approximately 1 min. Then, the water-reducing agent, which was diluted with water, along with about 3/4 of the total water, was added, and mixing continued for around 4 min. The mixture was then allowed to stand for about 30 s. Finally, the remaining 1/4 of the water was added, and mixing was carried out for an additional 3 min.

Once mixed, the concrete was poured into test molds of various sizes (e.g., 100 mm × 100 mm × 100 mm and 100 mm × 100 mm × 400 mm). After 24 h of curing, the molds were removed, and the specimens were cured in a standard curing room (20°C ± 2°C, 95% relative humidity) until the specified testing age was reached. Concrete specimens made with Portland cement were designated as OPCC, those with slag-modified Portland cement as SGCC, PG-modified SSC specimens as PGSSCC, and DG-modified SSC specimens as DGSSCC.

For the paste specimens, standard sand was used, and they were demolded after 24 h and cured in the standard curing room (20°C ± 2°C, 95% RH) until the testing age. The water-to-cement ratio was set at 0.4.

2.3 Experimental methods

2.3.1 Mechanical test

The mechanical properties of concrete were tested according to the Standard Test Methods for Physical and Mechanical Properties of Concrete (GB/T 50081-2019). For compressive strength testing, specimens with dimensions of 100 mm × 100 mm × 100 mm were used, while for flexural strength testing, specimens with dimensions of 100 mm × 100 mm × 400 mm were employed.

2.3.2 Sulphate erosion test

Sulfate and acid erosion experiments followed the guidelines outlined in related research (Kwasny et al., 2018; Gutberlet et al., 2015) and were conducted according to (GB/T 50082-2009). A 5% mass concentration sulfate solution was used, with a solution-to-specimen volume ratio of 10:1. To simulate continuous chemical exposure, the erosion solution was replaced weekly. In addition to the chemical attack evaluation, a blank control group was included, where concrete specimens were immersed in pure water to examine the mechanical performance of the four cementitious materials under standard conditions. All experiments were conducted at a constant temperature of 20°C. The compressive strength of the specimens was evaluated at exposure intervals of 0, 7, 28, 60, and 180 days, and the compressive strength retention was calculated using the following formula:

$$\text{Strength retention rate} = \frac{CS_n}{CS_0} \times 100\%$$

Where: CS_n indicated the compressive strength of the specimen after being immersed in the solution for n d; CS_0 indicated the compressive strength of the specimen before immersion in the solution.

2.3.3 Water absorption test

Concrete samples were tested according to the relevant standard of ASTM C642-21. The procedure involved drying the samples in an oven at 105°C for 24 h and recording their dry mass. The samples were then immersed in water for not less than 48 h and until two successive values of mass of the surface-dried sample at intervals of 24 h show an increase in mass of less than 0.5%. The water absorption percentage was calculated using the following equation:

$$\text{Prcentage of water absorbed} = \frac{(m_1 - m_0)}{m_0} \times 100\%$$

Where: m_0 represented the dry mass of the concrete specimens and m_1 represented the mass of the concrete saturated with water.

2.3.4 Isothermal calorimetry

The thermal evolution of the cement specimens during hydration was measured using an isothermal calorimeter (TAOPO, TAM Air, United States) at a testing temperature of 22°C ± 1°C. Cement and water were mixed in a water-to-cement ratio of 0.4, then placed into glass ampoules and inserted into the calorimeter for data collection.

2.3.5 X-ray diffraction (XRD)

Phase characterization of the cement specimens was conducted using a Bruker D8 Advance X-ray diffractometer (Germany), with a Cu-Kα radiation source. The scanning range was 5°–70° with a step size of 0.02°/s.

2.3.6 Scanning electron microscopy (SEM)

The microstructure and morphology of the paste samples were analyzed using scanning electron microscopy with JEOL JSM-IT700HR and TESCAN MIRA LMS Xplore 30 instruments. For this analysis, the freshly fractured surfaces of the cement samples were sputter-coated with a thin layer of gold for 30 s to ensure conductivity.

2.3.7 Integrated evaluation

SSC, a new type of high-performance cement, has garnered increasing attention for its advantages in terms of environmental impact, energy consumption, and economic cost compared to Portland cement. This study explores the potential of SSC as

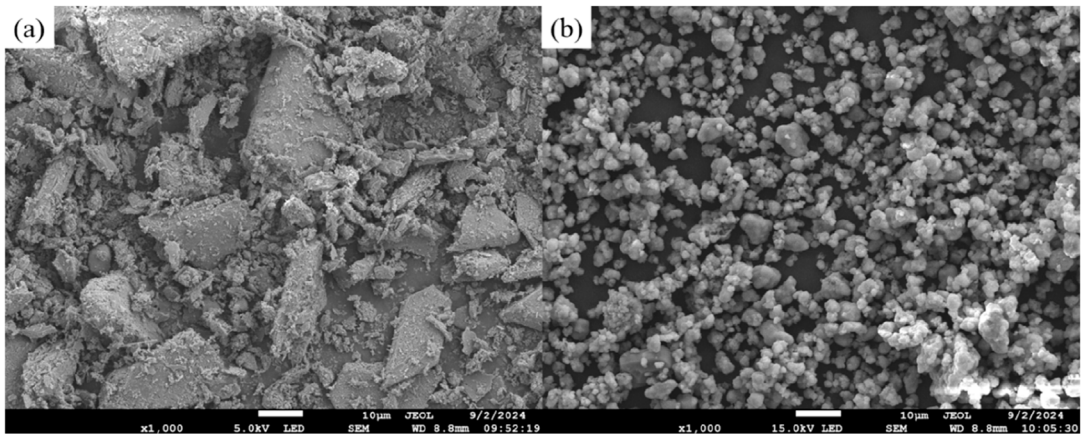

FIGURE 2
The micro-morphology of **(A)** PG and **(B)** DG.

TABLE 1 The chemical composition of cement, slag, PG and DG.

	Oxide	CaO	SiO_2	Al_2O_3	Fe_2O_3	SO_3	MgO	K_2O	Cl
Cement	wt%	55.45	22.62	8.1	3.30	2.75	2.36	1.67	-
Slag		43.21	30.22	15.56	0.27	2.36	6.65	0.56	-
PG		32.35	8.07	1.22	0.47	55.56	-	0.51	-
DG		46.45	0.32	0.35	0.42	43.86	1.05	1.99	4.7

TABLE 2 The formulation of concrete specimens.

	Oxide	Slag	PG	DG	Cement	CA	FA	Water	SP
OPCC	g	0	0	0	500	1,050	650	200	1
SGCC		250	0	0	250				2.5
PGSSCC		400	75	0	25				2.5
DGSSCC		400	0	75	25				2.5

a replacement for Portland cement by evaluating these three dimensions. The 28-day compressive strength was chosen as the performance index for the SSC hardened paste. Relative carbon emissions (RCE), relative energy consumption (REC), and relative cost (RC) were calculated using the following equations, providing a scientific foundation for the sustainable development of the industry.

$$RCE = \frac{CarbonEmission}{CompressiveStrength}$$

$$REC = \frac{EnergyConsumption}{CompressiveStrength}$$

$$RC = \frac{Cost}{CompressiveStrength}$$

3 Results and discussion

3.1 Mechanical performance

3.1.1 Compressive strength

Figure 3 presents the compressive strength of the different concrete specimens at various curing ages. Among all the specimens, SGCC exhibited the highest compressive strength across all curing times. At 3, 7, and 28 days, the compressive strengths of SGCC were 33.2 MPa, 48.5 MPa, and 59.2 MPa, respectively. In comparison, the compressive strength of OPCC was slightly lower, with values of 30 MPa, 45 MPa, and 56.3 MPa at the same curing times. PGSSCC showed a comparable trend, with compressive strengths of 27.3 MPa, 40.2 MPa, and 53.3 MPa at 3, 7, and 28 days, respectively.

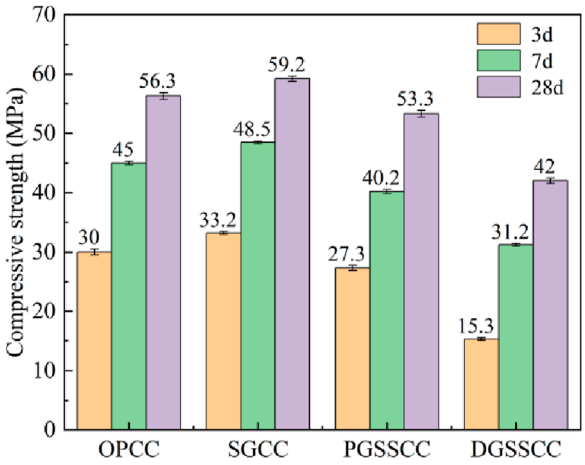

FIGURE 3
The compressive strength of different concrete specimens.

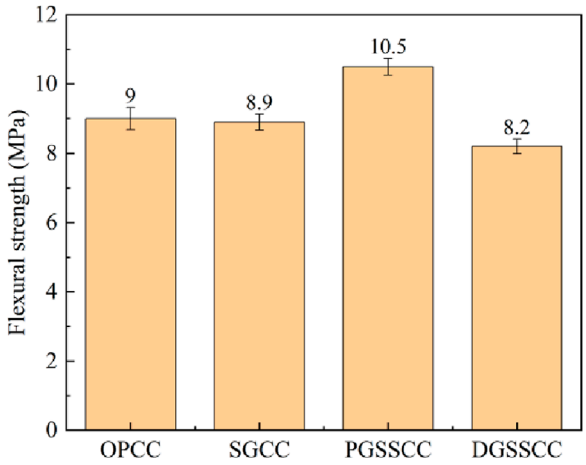

FIGURE 4
The flexural strength of different concrete specimens.

These values were similar to those of OPCC, though PGSSCC did not achieve the same strength levels as SGCC. On the other hand, DGSSCC exhibited significantly lower compressive strengths, with values of 15.3 MPa, 31.2 MPa, and 42 MPa at 3, 7, and 28 days, respectively.

The compressive strength results indicate that slag-modified cement (SGC) demonstrates excellent long-term strength development, which is consistent with previous findings (Islam et al., 2023). The addition of slag improves both the compressive and tensile strengths of concrete, which can be attributed to the chemical composition of slag, particularly its high content of CaO, SiO_2, and Al_2O_3. In an alkaline environment, these components of slag are activated and dissolve, producing C-S-H gels, which are crucial for strength development. Additionally, the aluminum phase in slag reacts with $CaSO_4$, forming AFt, which further enhances the strength and durability of the concrete. Moreover, the small and irregularly shaped slag particles help fill the voids between cement particles, improving the overall density and structure of the concrete. For SSC, the activation of slag is facilitated by sulfate activators such as PG and DG, which help form the same hydration products—AFt and C-S-H. In the case of PGSSCC, PG effectively activated the slag, promoting excellent strength development, although it did not reach the performance levels of SGCC. PG is known for its high sulfur content, which plays a critical role in the formation of AFt, contributing to the concrete's strength and durability.

In contrast, the activation effect of DG in DGSSCC was less pronounced. Despite its ability to activate slag, DG did not exhibit the same efficiency as PG. This can be attributed to the lower sulfur content in DG, which may not provide sufficient sulfate ions to ensure the stable formation of AFt. As a result, the compressive strength of DGSSCC was notably lower compared to PGSSCC and SGCC, particularly at later curing ages.

3.1.2 Flexural strength

The evaluation of flexural strength is crucial in assessing the tensile resistance of concrete, particularly since this property is directly related to the material's performance under bending stresses in practical applications. As shown in Figure 4, the flexural strength of concrete specimens typically ranged between 10% and 20% of their compressive strength, highlighting the inherent mechanical performance variations between different concrete types. Among all the tested specimens, PGSSCC exhibited the highest flexural strength, achieving 10.5 MPa at 28 days of curing. This superior performance can be attributed to the substantial formation of AFt in the hydration products of PGSSCC. AFt is known for its densified microstructure and superior bonding properties, which significantly enhance the toughness and cracking resistance of concrete. The presence of a high volume of AFt likely contributes to the improved flexural strength by enhancing the concrete's ability to resist tensile stresses and prevent cracks from propagating under bending loads.

Following PGSSCC, OPCC showed a flexural strength of 9 MPa at 28 days. While slightly lower than that of PGSSCC, this value still indicates relatively good structural performance. OPCC's behavior is consistent with expectations for conventional cements, which generally maintain stability during service but typically exhibit lower resistance to bending compared to advanced cementitious materials like PGSSCC. SGCC exhibited a flexural strength of 8.9 MPa at 28 days, which was slightly lower than that of OPCC. This result suggests that SGCC maintains good structural integrity under these mix conditions, but its flexural performance still lags behind that of PGSSCC. The hydration products in SGCC are primarily influenced by slag, which, while providing significant long-term strength development, does not contribute to as much improvement in flexural strength as AFt in PGSSCC. Lastly, DGSSCC showed the lowest flexural strength at 8.2 MPa at 28 days. The reduced performance can be attributed to the different hydration products formed in DGSSCC, as compared to PGSSCC. It is likely that the lower sulfur content in DG resulted in a less efficient activation of the slag, which in turn led to a reduced formation of AFt. Consequently, DGSSCC did not achieve the same level of bonding and densification in its microstructure as PGSSCC, which impacted its flexural strength.

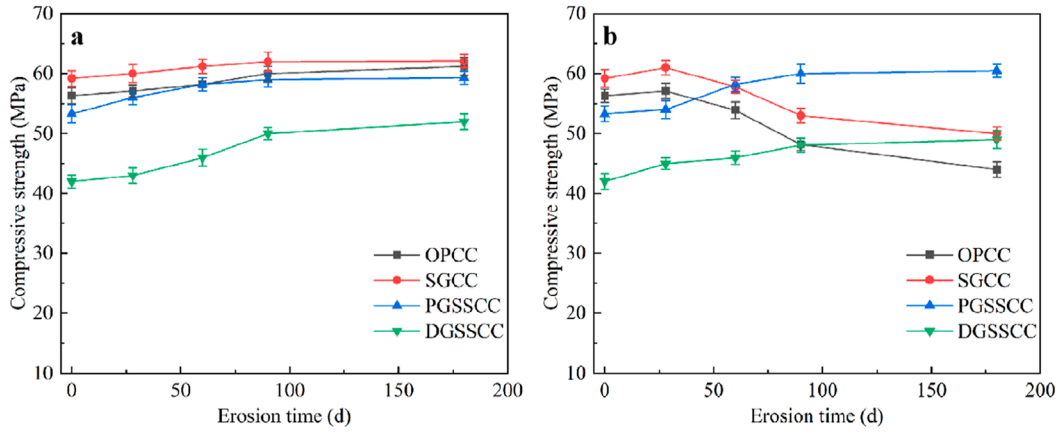

FIGURE 5
The compressive strength of different concrete specimens with time of immersion in **(A)** pure water and **(B)** Na_2SO_4 solution.

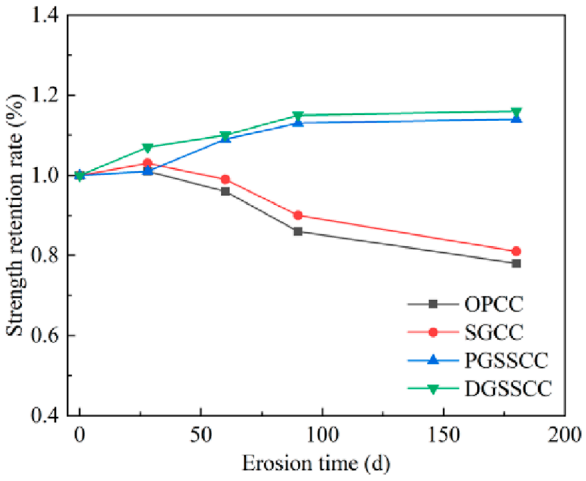

FIGURE 6
The retention of compressive strength of concrete specimens attacked by sulfate.

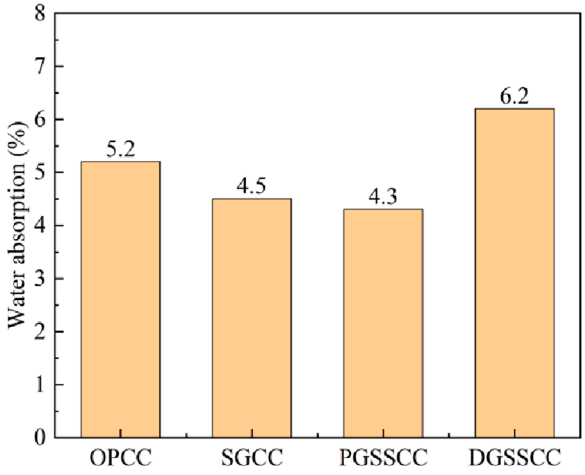

FIGURE 7
The water absorption of different concrete specimens after 28 days of standard curing.

3.2 Resistant to sulfate attack

The compressive strength of different concrete specimens after immersion in pure water and Na_2SO_4 solution over time is shown in Figure 5. Figure 5A demonstrates that the compressive strength of all concrete specimens immersed in pure water increased over time, suggesting that exposure to pure water did not lead to any degradation of concrete strength. This behavior is typical of concrete curing, where continued hydration in pure water contributes to strength development. In contrast, Figure 5B presents the behavior of the concrete specimens immersed in a 5% Na_2SO_4 solution. Initially, there was a slight increase in compressive strength for all specimens after 28 days of immersion. However, after 60 days, distinct differences in performance became evident. OPCC and SGCC exhibited a reduction in compressive strength, with SGCC showing a slower rate of deterioration compared to OPCC. Notably, PGSSCC and DGSSCC demonstrated no reduction in compressive strength even after 60 days of exposure, indicating superior resistance to sulfate attack.

Figure 6 further illustrates the retention of compressive strength of concrete specimens exposed to sulfate attack. While OPCC and SGCC experienced a clear decline in strength, PGSSCC and DGSSCC retained their strength, reinforcing the notion that SSC provides significantly better sulfate resistance compared to OPCC and SGCC.

This discrepancy in performance can primarily be attributed to the composition of the hydration products. During the hydration of SSC, the dominant products are AFt and C-S-H gels, which have a relatively low pH and do not produce $Ca(OH)_2$ as in conventional cements. In traditional Portland cements, $Ca(OH)_2$ reacts with Na_2SO_4 in the sulfate solution to form $CaSO_4$, which is insoluble in water, leading to the degradation of concrete strength. Additionally, the formation of expansive gypsum due to this reaction may cause volumetric changes and cracking, further

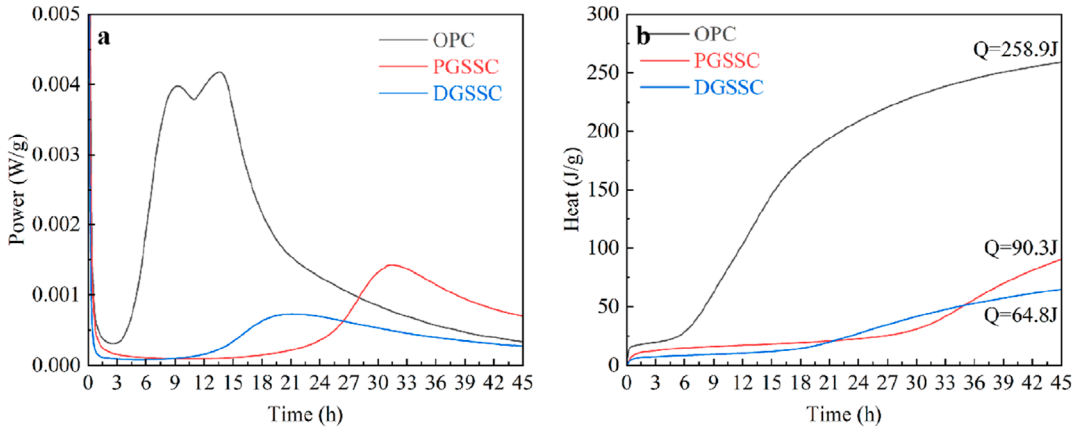

FIGURE 8
The thermal hydration curves of OPC, PGSSC and DGSSC: **(A)** heat flow; **(B)** cumulative heat.

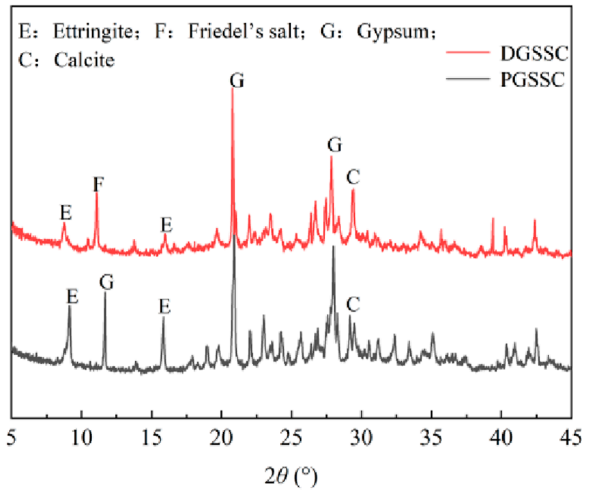

FIGURE 9
The phase composition of OPC, PGSSC and DGSSC.

weakening the concrete structure. Therefore, the superior sulfate corrosion resistance of SSC concrete stems from the selectivity of its hydration products and its favorable strength development behavior, which allows it to maintain its strength even under harsh environmental conditions. These characteristics position SSC as a promising material for environments prone to chemical corrosion, offering significant potential for specialized projects requiring enhanced durability. In particular, SSC's performance in sulfate-rich environments demonstrates its advantages over traditional cement systems, providing new opportunities to overcome the limitations of conventional cements.

3.3 Water absorption

Figure 7 presents the water absorption characteristics of the different concrete specimens after 28 days of standard curing. It is evident that PGSSCC exhibited the lowest water absorption, suggesting that it possesses the highest density among all the specimens. High-density concrete is not only beneficial in resisting water ingress but also offers better protection against chemical attacks. In road construction, concrete surfaces are continuously exposed to sunlight and various chemical agents. Concrete with lower water absorption significantly enhances resistance to UV radiation and chemical erosion, playing a crucial role in prolonging the service life of the pavement.

Figure 7 further highlights that water absorption in concrete also influences surface roughness and skid resistance. The appropriate level of water absorption can improve the frictional properties of the concrete surface, which is critical for ensuring road safety. Lower water absorption correlates with reduced risk of slippage, thus enhancing vehicle stability and reducing the likelihood of traffic accidents. Consequently, controlling the water absorption of concrete is paramount in road paving applications. The formation of C-S-H, a key product in the hydration of concrete, plays a decisive role in both the strength and durability of the material. During the hydration process, C-S-H gels fill the pores in the concrete, compacting the microstructure and reducing water absorption. This compaction not only improves the compressive strength but also contributes to the concrete's corrosion resistance, thus ensuring a long service life. In the case of SSC, which contains a higher proportion of C-S-H in its hydration products compared to Portland cement, the material shows a more efficient regulation of water absorption. This results in superior performance, making SSC a promising alternative for concrete with both enhanced durability and reduced water permeability.

3.4 Hydration mechanism of SSC

The thermal hydration curves of OPC, PG-modified SSC (PGSSC), and DG-modified SSC (DGSSC) are presented in Figure 8. The data reveal that the induction period of SSC was notably longer than that of OPC, a phenomenon attributed to the higher content of waste gypsum in SSC. Additionally, while OPC exhibited two distinct exothermic peaks, PGSSC and DGSSC showed only one. The initial peak observed in OPC represents the rapid generation

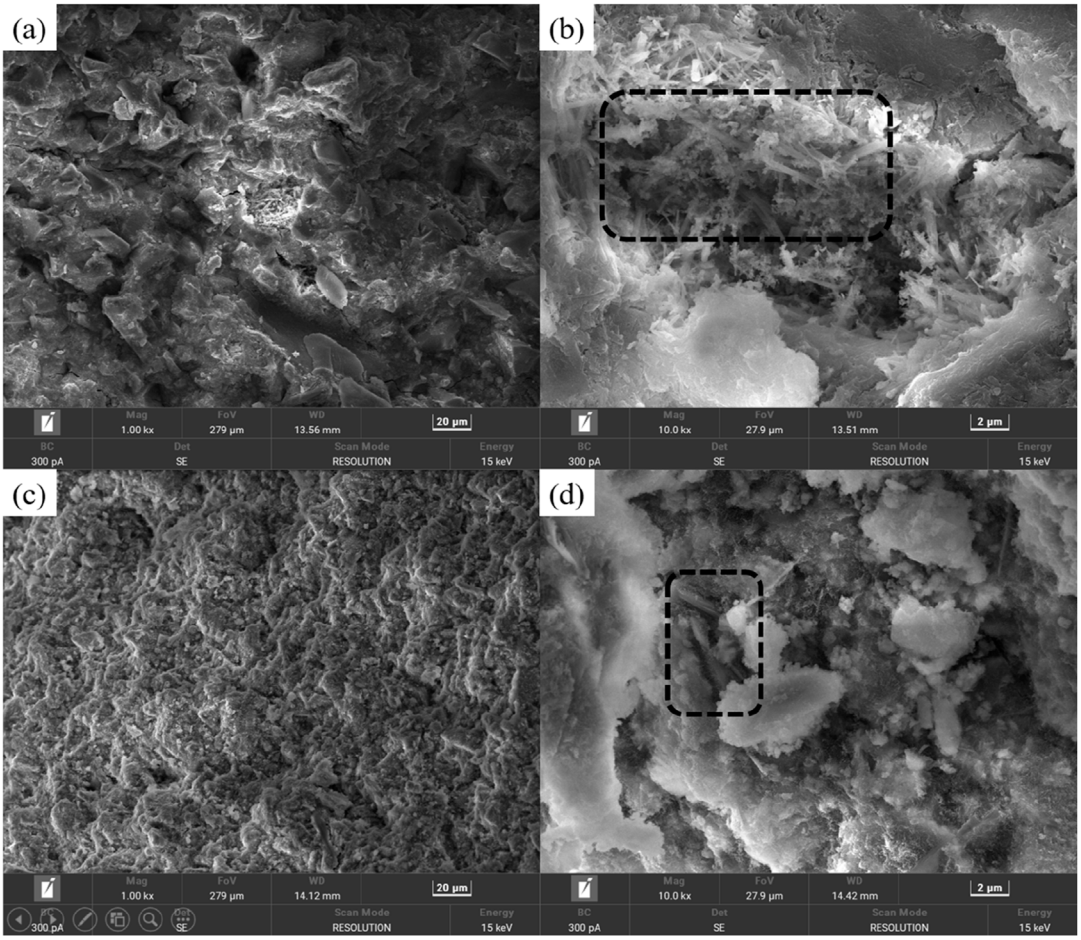

FIGURE 10
The SEM images of **(A, B)** PGSSC and **(C, D)** DGSSC.

TABLE 3 The carbon emission, energy consumption and cost of different raw materials production.

	Carbon emissions (kg CO_2-eq/kg)	Energy (MJ/Kg)	Cost (CNY/Kg)
Cement	1.17	6.46	0.38
Slag	0.052	1.3	0.28
PG	0.223	0.692	0.512
DG	0.246	0.685	0.494
SP	0.72	0.329	2.75
Water	0.0003	0.0002	0.005

of C-S-H, the primary strength-forming phase. The subsequent peak reflects the depletion of SO_4^{2-} during hydration. In contrast, the single exothermic peak in SSC indicates that the slag in SSC was activated by alkaline conditions to form C-S-H and AFt, primarily in the presence of $CaSO_4$. This differs from OPC, where $Ca(OH)_2$ is released and contributes to the formation of expansive compounds.

The heat flow curves also show that the hydration rate of SSC was lower than that of OPC, reflecting a slower reaction process. The total heat released by the hydration process of OPC at 45 h was 258.9 J, significantly higher than that of PGSSC (90.3 J) and DGSSC (64.8 J), as shown in Figure 8B. This lower thermal release in SSC is indicative of a slower, more controlled hydration process, which may contribute to the material's longer-term strength development.

Further analysis of the phase composition of the hydration products is shown in Figure 9, where PGSSC primarily contained AFt, gypsum, and calcium carbonate. In contrast, DGSSC exhibited additional phases, including Friedel's salt, a form of the AFm

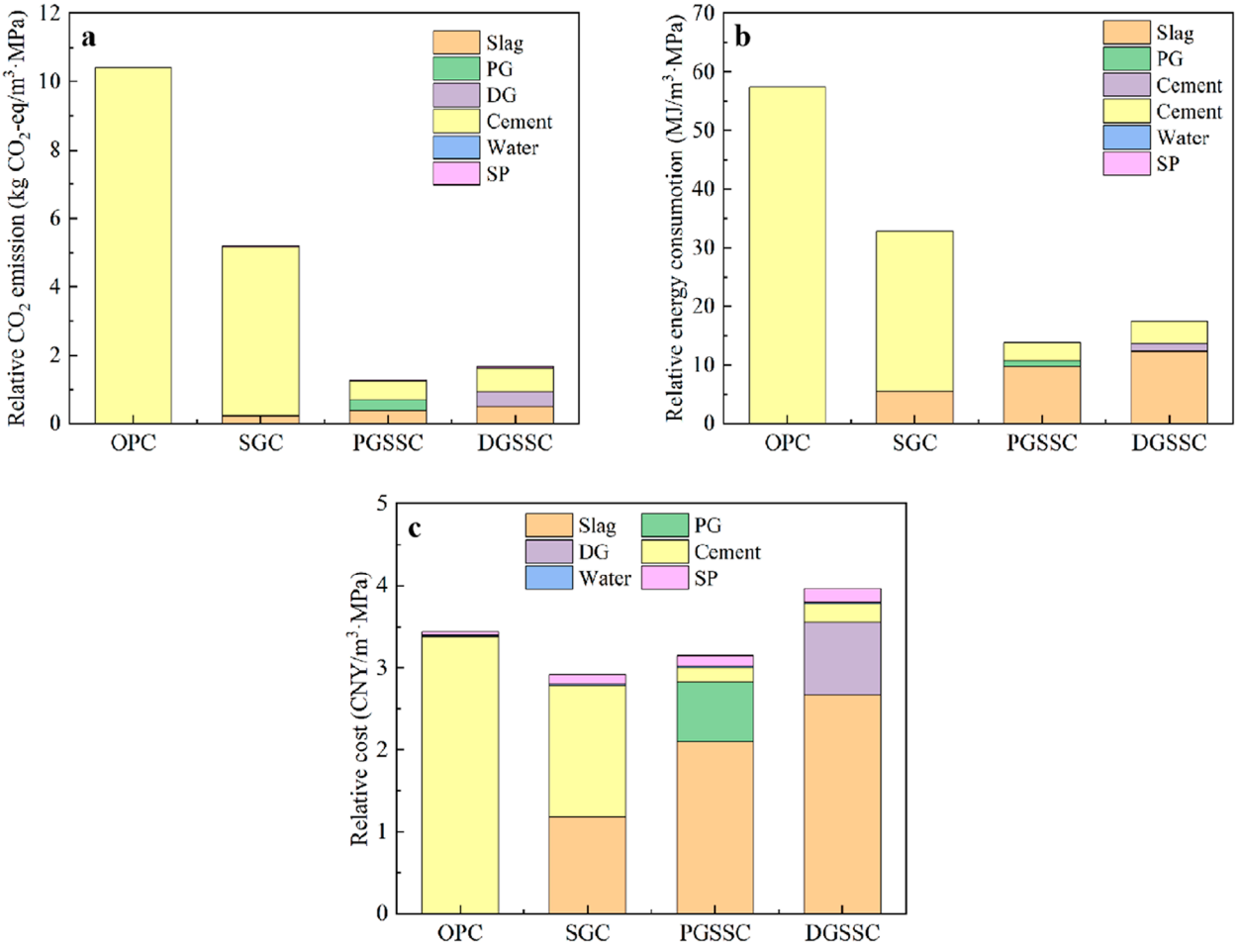

FIGURE 11
The **(A)** RCE, **(B)** REC and **(C)** RC values of various cementitious materials.

phase, which likely results from the small amount of Cl^- present, converting some of the AFt to Friedel's salt. The presence of $CaCO_3$ can be attributed to the unavoidable carbonation of the specimens during curing.

Significantly, the absence of $Ca(OH)_2$ in SSC is notable, suggesting that this compound was consumed during the reaction of slag with the alkaline activators, unlike in traditional Portland cement systems where $Ca(OH)_2$ remains prevalent. This absence of $Ca(OH)_2$ further contributes to the environmentally friendly nature of SSC, as it reduces the release of lime-based compounds into the environment.

The microstructural characteristics of PGSSC and DGSSC were observed using SEM, as shown in Figure 10. Figures 10A, C indicate that the microstructure of DGSSC was more porous and fluffy compared to PGSSC, suggesting a less compact structure in DG-modified SSC. Both PGSSC and DGSSC exhibited morphology consistent with their gypsum content, underscoring the importance of gypsum in the hydration process. AFt (Figure 10B) was clearly observed in both materials, filling the pores and acting to bond the microstructure, contributing to the overall strength. However, DGSSC exhibited small, flaky crystals, consistent with the presence of Friedel's salt, aligning with the phase composition analysis.

3.5 Integrated evaluation of SSC

To evaluate the environmental and economic impacts of SSC, we analyzed the carbon emissions, energy consumption, and production cost of different raw materials based on results from related studies (Xiao et al., 2021; Du et al., 2023; Cui et al., 2018) (Table 3). The evaluation focused on the cementitious materials, as the differences in performance between the concrete specimens were attributed mainly to the composition of these materials. The carbon emissions, energy consumption, and costs associated with different materials were calculated, and the RCE, REC, and RC values of various materials at 28 days of curing are depicted in Figure 11.

Figure 11 presents the RCE, REC, and RC values for various cementitious materials. Compared to OPC, increasing the slag content in the mix significantly reduced both RCE and REC, particularly for SSC. Specifically, the RCE, REC, and RC of SGC were reduced by 50.1%, 42.8%, and 15.1%, respectively. The RCE, REC, and RC of PGSSC were reduced by 87.6%, 75.9%, and 8.6%, respectively. The RCE and REC of DGSSC were reduced by 83.9% and 69.6%, respectively, though the RC was higher than that of OPC due to the higher cost of DG.

This data clearly demonstrates that SSC has a significant advantage in terms of reducing carbon emissions and energy consumption. However, the production cost of SSC is still higher, primarily due to the cost of raw materials like PG and DG, which are more expensive than traditional Portland cement. The production technology for SSC needs further optimization to reduce its cost and make it a more economically viable alternative in the construction industry. The analysis of specific components' contribution to these parameters reveals that cement production is the major contributor to carbon emissions and energy consumption. As shown in Figures 11A, B, the carbon emissions and energy consumption from cement production are significantly higher compared to slag and waste gypsum, which have minimal environmental impact. Therefore, reducing the cement content in SSC mixtures could be an effective strategy to further decrease carbon emissions and energy consumption.

PGSSC exhibits the lowest RCE and REC, owing to its superior performance in terms of strength, while DGSSC has slightly higher values due to lower strength development. Figure 11C illustrates that the cost of DGSSC was the highest, indicating that cost optimization strategies for SSC are necessary. By refining the production process, it may be possible to reduce the cost of DGSSC, making SSC a more cost-effective and environmentally friendly alternative to traditional cement.

4 Conclusion

This study investigated the mechanical performance, corrosion resistance, and water absorption properties of SSCC, OPCC, and SGCC through a series of macroscopic experiments. Additionally, the hydration mechanisms of SSC and OPC were explored to provide insights into the observed differences. The key conclusions drawn from this research are as follows:

1. PGSSCC exhibited excellent mechanical performance, with compressive strengths of 27.3 MPa, 40.2 MPa, and 53.3 MPa at 3 days, 7 days, and 28 days, respectively. The mechanical performance of PGSSCC was superior to that of DGSSCC, highlighting the more effective activation of slag by PG compared to DG. Furthermore, when comparing the sulfate resistance of SSCC with OPCC, it was found that SSCC demonstrated significantly better resistance to sulfate attack, underscoring its durability in aggressive environments.
2. Thermal hydration tests revealed that the hydration exothermic heat of SSC was notably lower than that of OPC. The hydration products of PG-modified SSC primarily consisted of AFt and C-S-H. A key distinction between SSC and OPC was the near absence of $Ca(OH)_2$ in SSC hydration products. Additionally, the microstructure of PGSSCC was found to be more densified than that of DGSSCC, which contributed to better interfacial adhesion and enhanced mechanical performance of PGSSCC.
3. In terms of sustainability, the integrated evaluation showed that PGSSCC had the lowest carbon emissions and energy consumption, significantly outperforming OPCC. Furthermore, the relative cost of PGSSCC was also lower than that of OPCC, indicating that SSCC not only enhances the corrosion resistance of concrete but also offers environmental and economic benefits. The reduction in carbon emissions and energy consumption associated with SSC makes it a promising alternative for road concrete, offering substantial improvements in both sustainability and durability.

In summary, this study presents innovative approaches for reducing carbon emissions in road concrete. The superior corrosion resistance of SSC makes it particularly suitable for use in aggressive environments, providing long-term durability. However, the relatively poor carbonation resistance of SSC remains a limitation for its widespread adoption. Further research into enhancing the carbonation resistance of SSC will be crucial for optimizing its performance and achieving the goal of reducing carbon emissions in road construction. Additionally, the performance of SSCC is influenced by the specific mineral phases and their content in PG and DG, suggesting that further exploration into the optimization of these materials is necessary to improve the overall properties of SSCC.

Data availability statement

The original contributions presented in the study are included in the article/supplementary material, further inquiries can be directed to the corresponding author.

Author contributions

HW: Investigation, Writing–original draft. FX: Methodology, Writing–review and editing. ZL: Methodology, Writing–original draft. SZ: Data curation, Formal Analysis, Writing–review and editing. EX: Data curation, Formal Analysis, Writing–original draft. YY: Investigation, Writing–original draft. YZ: Supervision, Writing–review and editing. CL: Supervision, Writing–original draft.

Funding

The author(s) declare that financial support was received for the research, authorship, and/or publication of this article. This work was supported by Tianjin Philosophy and Social Sciences Planning Project, China (TJYJ24-001).

Conflict of interest

Authors HW, ZL, and EX were employed by Cangzhou Qugang Expressway Construction Co. Ltd. Author SZ was employed by Fujian Zhanglong Construction Investment Group Co. Ltd. Author YY was employed by Fujian Xingyan Construction Group Co. Ltd. Author YY was employed by Fujian Rongguan Construction Engineering Co. Ltd. Author YZ was employed by China MCC22 Group Corporation Ltd.

The remaining authors declare that the research was conducted in the absence of any commercial or financial relationships that could be construed as a potential conflict of interest.

Generative AI statement

The authors declare that no Generative AI was used in the creation of this manuscript.

Publisher's note

All claims expressed in this article are solely those of the authors and do not necessarily represent those of their affiliated organizations, or those of the publisher, the editors and the reviewers. Any product that may be evaluated in this article, or claim that may be made by its manufacturer, is not guaranteed or endorsed by the publisher.

References

Akkaya, A., and Çağatay, İ. H. (2021). Experimental investigation of the use of pervious concrete on high volume roads. *Constr. Build. Mater.* 279, 122430. doi:10.1016/j.conbuildmat.2021.122430

Blanco, C. C. (2022). A classification of carbon abatement opportunities of global firms. *Manuf. and Serv. Operations Manag.* 24 (5), 2648–2665. doi:10.1287/msom.2022.1115

Cabrera-Luna, K., Maldonado-Bandala, E. E., Nieves-Mendoza, D., Castro-Borges, P., and Escalante García, J. I. (2020). Novel low emissions supersulfated cements of pumice in concrete; mechanical and electrochemical characterization. *J. Clean. Prod.* 272, 122520. doi:10.1016/j.jclepro.2020.122520

Cabrera-Luna, K., Perez-Cortes, P., and Escalante Garcia, J. I. (2024). Influence of quicklime and Portland cement, as alkaline activators, on the reaction products of supersulfated cements based on pumice. *Cem. Concr. Compos.* 146, 105379. doi:10.1016/j.cemconcomp.2023.105379

Cantini, A., Leoni, L., De Carlo, F., Salvio, M., Martini, C., and Martini, F. (2021). Technological energy efficiency improvements in cement industries. *Sustainability* 13, 3810. doi:10.3390/su13073810

Chang, S., Gao, F., Wang, L., Jin, Q., Liu, S., and Wan, L. (2024). Deterioration mechanism of supersulfated cement paste exposed to sulfate attack and combined acid-sulfate attack. *Constr. Build. Mater.* 414, 134978. doi:10.1016/j.conbuildmat.2024.134978

Cui, L., Li, Y., Tang, Y., Shi, Y., Wang, Q., Yuan, X., et al. (2018). Integrated assessment of the environmental and economic effects of an ultra-clean flue gas treatment process in coal-fired power plant. *J. Clean. Prod.* 199, 359–368. doi:10.1016/j.jclepro.2018.07.174

Cui, W., Liu, J., Duan, W., Xie, M., Li, X., and Dong, X. (2024). Study on the synergistic effects and eco-friendly performance of red mud-based quaternary cementitious materials. *Constr. Build. Mater.* 428, 136352. doi:10.1016/j.conbuildmat.2024.136352

Du, J., Wang, Y., Bao, Y., Sarkar, D., and Meng, W. (2023). Valorization of wasted-derived biochar in ultra-high-performance concrete (UHPC): pretreatment, characterization, and environmental benefits. *Constr. Build. Mater.* 409, 133839. doi:10.1016/j.conbuildmat.2023.133839

Gartner, E. (2004). Industrially interesting approaches to "low-CO_2" cements. *Cem. Concr. Res.* 34 (9), 1489–1498. doi:10.1016/j.cemconres.2004.01.021

Gracioli, B., Angulski da Luz, C., Beutler, C. S., Pereira Filho, J. I., Frare, A., Rocha, J. C., et al. (2020). Influence of the calcination temperature of phosphogypsum on the performance of supersulfated cements. *Constr. Build. Mater.* 262, 119961. doi:10.1016/j.conbuildmat.2020.119961

Gutberlet, T., Hilbig, H., and Beddoe, R. E. (2015). Acid attack on hydrated cement — effect of mineral acids on the degradation process. *Cem. Concr. Res.* 74, 35–43. doi:10.1016/j.cemconres.2015.03.011

Huang, Y., Qian, J., Lu, L., Zhang, W., Wang, S., Wang, W., et al. (2020). Phosphogypsum as a component of calcium sulfoaluminate cement: hazardous elements immobilization, radioactivity and performances. *J. Clean. Prod.* 248, 119287. doi:10.1016/j.jclepro.2019.119287

Intergovernmental Panel on Climate Change (2022). *Global warming of 1.5°C: IPCC special report on impacts of global warming of 1.5°C above pre-industrial levels in context of strengthening response to climate change, sustainable development, and efforts to eradicate poverty*. Cambridge: Cambridge University Press.

Islam, A. B. M. S., Arifuzzaman, M., Gul Muhammad, A., Gazder, U., Tito Mokammel, H., and Uddin, M. A. (2023). Slag: a sustainable alternative for Portland cement concrete. *IET Conf. Proc.* 44, 190–193. doi:10.1049/icp.2024.0923

Jiang, J., Sui, S., Liu, Z., Wang, F., and Geng, G. (2024). Research on silicoaluminate-based low-carbon cementitious material—a state-of-the-art review. *Fundam. Res.* doi:10.1016/j.fmre.2024.04.020

Jiang, L., Li, C., Wang, C., Xu, N., and Chu, H. (2018). Utilization of flue gas desulfurization gypsum as an activation agent for high-volume slag concrete. *J. Clean. Prod.* 205, 589–598. doi:10.1016/j.jclepro.2018.09.145

Kang, Z., Zhang, J., Li, N., Lv, T., Yang, Y., and Lu, J. (2024). Utilization of biochar as a green additive in supersulfated cement: properties, mechanisms, and environmental impacts. *Constr. Build. Mater.* 445, 137923. doi:10.1016/j.conbuildmat.2024.137923

Kazanskaya, L. F., Smirnova, O. M., Palomo, Á., Menendez Pidal, I., and Romana, M. (2021). Supersulfated cement applied to produce lightweight concrete. *Mater. (Basel)* 14, 403. doi:10.3390/ma14020403

Kwasny, J., Aiken, T. A., Soutsos, M. N., McIntosh, J. A., and Cleland, D. J. (2018). Sulfate and acid resistance of lithomarge-based geopolymer mortars. *Constr. Build. Mater.* 166, 537–553. doi:10.1016/j.conbuildmat.2018.01.129

Lantsoght, E. O. L. (2022). Advanced structural concrete materials in bridges. *Mater. (Basel)* 15, 8346. doi:10.3390/ma15238346

Li, M., Zhang, M., Du, C., and Chen, Y. (2020a). Study on the spatial spillover effects of cement production on air pollution in China. *Sci. Total Environ.* 748, 141421. doi:10.1016/j.scitotenv.2020.141421

Li, X., Zhou, Y., Shi, Y., and Zhu, Q. (2023). Fluoride immobilization and release in cemented PG backfill and its influence on the environment. *Sci. Total Environ.* 869, 161548. doi:10.1016/j.scitotenv.2023.161548

Li, Y., Qiao, C., and Ni, W. (2020b). Green concrete with ground granulated blast-furnace slag activated by desulfurization gypsum and electric arc furnace reducing slag. *J. Clean. Prod.* 269, 122212. doi:10.1016/j.jclepro.2020.122212

Lin, J., Dong, Y., Duan, J., Zhang, D., and Zheng, W. (2021). Experiment on single-tunnel fire in concrete immersed tunnels. *Tunn. Undergr. Space Technol.* 116, 104059. doi:10.1016/j.tust.2021.104059

Liu, S., Fang, P., Ren, J., and Li, S. (2020). Application of lime neutralised phosphogypsum in supersulfated cement. *J. Clean. Prod.* 272, 122660. doi:10.1016/j.jclepro.2020.122660

Liu, S., Wang, L., and Yu, B. (2019). Effect of modified phosphogypsum on the hydration properties of the phosphogypsum-based supersulfated cement. *Constr. Build. Mater.* 214, 9–16. doi:10.1016/j.conbuildmat.2019.04.052

Mo, K. H., Alengaram, U. J., Jumaat, M. Z., Yap, S. P., and Lee, S. C. (2016). Green concrete partially comprised of farming waste residues: a review. *J. Clean. Prod.* 117, 122–138. doi:10.1016/j.jclepro.2016.01.022

Peng, Z., Zhou, Y., Wang, J., Chen, L., and Miao, C. (2022). The impediment and promotion effects and mechanisms of lactates on the hydration of supersulfated cements - aiming at a performance enhancement. *J. Clean. Prod.* 341, 130751. doi:10.1016/j.jclepro.2022.130751

Pinto, S. R., Angulski da Luz, C., Munhoz, G. S., and Medeiros-Junior, R. A. (2020a). Resistance of phosphogypsum-based supersulfated cement to carbonation and chloride ingress. *Constr. Build. Mater.* 263, 120640. doi:10.1016/j.conbuildmat.2020.120640

Pinto, S. R., Angulski da Luz, C., Munhoz, G. S., and Medeiros-Junior, R. A. (2020b). Durability of phosphogypsum-based supersulfated cement mortar against external attack by sodium and magnesium sulfate. *Cem. Concr. Res.* 136, 106172. doi:10.1016/j.cemconres.2020.106172

Selvam, M., Kumar, M. N., and Singh, S. (2023). Comparative analysis of jointed plain concrete pavement and roller-compacted concrete pavement. *Transp. Res. Rec.* 2678 (5), 196–210. doi:10.1177/03611981231188722

Wang, F., Du, H., Zheng, Z., Xu, D., Wang, Y., Li, N., et al. (2024). The impact of fly ash on the properties of cementitious materials based on slag-steel slag-gypsum solid waste. *Mater. (Basel)* 17, 4696. doi:10.3390/ma17194696

Wang, Y., Pan, Z., Zhao, C., and Zeng, B. (2023). Long-term behavior of prestressed concrete industrial buildings in chloride-based industrial environments. *J. Build. Eng.* 76, 107344. doi:10.1016/j.jobe.2023.107344

Wu, M., Zhang, Y., Liu, G., Wu, Z., Yang, Y., and Sun, W. (2018). Experimental study on the performance of lime-based low carbon cementitious materials. *Constr. Build. Mater.* 168, 780–793. doi:10.1016/j.conbuildmat.2018.02.156

Wu, Q., Xue, Q., and Yu, Z. (2021). Research status of super sulfate cement. *J. Clean. Prod.* 294, 126228. doi:10.1016/j.jclepro.2021.126228

Xiao, B., Wen, Z., Miao, S., and Gao, Q. (2021). Utilization of steel slag for cemented tailings backfill: hydration, strength, pore structure, and cost analysis. *Case Stud. Constr. Mater.* 15, e00621. doi:10.1016/j.cscm.2021.e00621

Xu, F., Lin, X., and Zhou, A. (2021). Performance of internal curing materials in high-performance concrete: a review. *Constr. Build. Mater.* 311, 125250. doi:10.1016/j.conbuildmat.2021.125250

Xue, Y., Liu, C., Shi, Q., Ju, Z., Fan, G., Zhang, C., et al. (2024). Road performance and mechanism of Hot in-place recycling asphalt mixture modified by direct-to-plant SBS. *Constr. Build. Mater.* 416, 135122. doi:10.1016/j.conbuildmat.2024.135122

Zhang, Y. (2021). Modeling of thermal expansion characteristics of concrete in agricultural water conservancy projects. *Arabian J. Geosciences* 14 (7), 575. doi:10.1007/s12517-021-06896-9

Zhonglin, L., Ye, X., Cheng, L., Biao, P., Yibing, L., Weiguang, Z., et al. (2024). Investigation on the compressive strength of desulfurization gypsum binary cementitious materials with low energy consumption: the utilization enhancement of industrial wastes. *Case Stud. Constr. Mater.* 21, e03582. doi:10.1016/j.cscm.2024.e03582

Zokaei, S., Siad, H., Lachemi, M., Mahmoodi, O., Ozcelikci, E., and Şahmaran, M. (2024). Engineered cementitious composites with super-sulfated cement: mechanical, physical, and durability performance. *Mater. (Basel)* 17, 2240. doi:10.3390/ma17102240